Amino Acids (2012) 42:117–128
DOI 10.1007/s00726-010-0640-1

REVIEW ARTICLE

Protein damage by photo-activated Zn(II) *N*-alkylpyridylporphyrins

Ludmil Benov · James Craik · Ines Batinic-Haberle

Received: 3 December 2009 / Accepted: 22 May 2010 / Published online: 18 June 2010

Abstract Destruction of unwanted cells and tissues in photodynamic therapy (PDT) is achieved by a combination of light, oxygen, and light-sensitive molecules. The advantages of PDT compared to other traditional treatment modalities, and the shortcomings of the currently used photosensitizers, have stimulated the search for new, more efficient photosensitizer candidates. Ability to inflict selective damage to particular proteins through photo-irradiation would significantly advance the design of highly specific photosensitizers. Achieving this objective requires comprehensive knowledge concerning the interactions of the particular photosensitizer with specific targets. Here, we summarize the effects of Zn(II) *N*-alkylpyridylporphyrin-based photosensitizers on intracellular (metabolic, antioxidant and mitochondrial enzymes) and membrane proteins. We emphasize how the structural modifications of the porphyrin side substituents affect their lipophilicity, which in turn influence their subcellular localization. Thus, Zn(II) *N*-alkylpyridylporphyrins target particular cellular sites and proteins of interest, and are more efficient than hematoporphyrin D, whose commercial preparation (Photofrin) has been clinically approved for PDT.

Keywords *Ortho*, *meta*, and *para* isomeric Zn(II) *N*-alkylpyridyl porphyrins · Photosensitizer · Hematoporphyrin D (HpD) · Oxidative protein modification · Photodynamic therapy

L. Benov (✉) · J. Craik
Department of Biochemistry, Faculty of Medicine, Kuwait University, P. O. Box 24923, 13110 Safat, Kuwait
e-mail: lbenov@hsc.edu.kw

I. Batinic-Haberle
Department of Radiation Oncology, Duke University Medical Center, Durham, NC 27710, USA

Introduction

Photodynamic therapy (PDT) is emerging as a promising treatment for both neoplastic and non-neoplastic disorders. It has been successfully used for the elimination of tumors (Castano et al. 2006; Juarranz et al. 2008; Robertson et al. 2009), new blood vessels (Chen et al. 2006), and atherosclerotic plaques (Waksman et al. 2008; Woodburn et al. 1996), for the treatment of skin diseases (Silva et al. 2008; Taub 2007), and killing of pathogenic microorganisms (Donnelly et al. 2008). The destruction of cells and tissues is achieved by a combination of light, oxygen, and light-sensitive photosensitizer (PS). Ideally, a PS should localize in the target cells and tissues, and upon illumination, produce cytotoxic reactive species.

Photophysics and photochemistry

In its ground state, the photosensitizer has two electrons with opposite spins (singlet state) in the low energy molecular orbital. The energy of light absorbed by the PS molecule lifts one of those electrons into a high-energy orbital without changing its spin. This short-lived (nanoseconds) state is the first excited singlet state of the PS. A PS molecule can lose its energy by emitting light (fluorescence), or internal conversion into heat. Alternatively, the spin of the excited electron can be inverted by intersystem crossing to form an excited triplet PS state where the two electrons have parallel spins. The lifetime of the triplet state is much longer (microseconds), because the direct return of the electron to the low energy molecular orbital is spin forbidden.

While in the excited triplet state, the PS can participate in two types of processes, known as Type 1 and Type 2

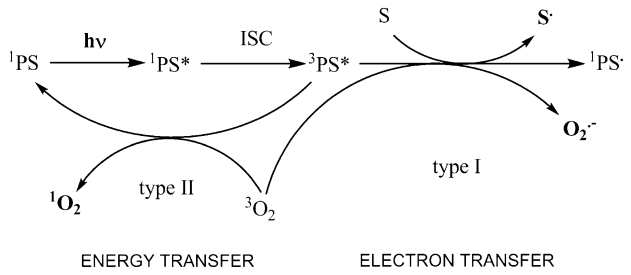

Fig. 1 Generation of reactive species by photosensitizers (PS). *^1PS* PS molecule in its ground (singlet) state having two electrons with opposite spins, *^1PS** first excited singlet state of the PS, *ISC* intersystem crossing—the spin of the excited electron is inverted, *^3PS** excited triplet PS state—the two electrons have parallel spins, *S* any molecule in the environment, participating in redox reaction with ^{3}PS*, *$^1PS^{\cdot}$* and *S*· free radicals formed as a result of the redox reaction, *$^1O_2$* singlet oxygen, *$^3O_2$* oxygen in its ground (triplet) state, *$O_2^{\cdot-}$* superoxide anion radical

(Foote 1991) (Fig. 1). In Type 1 processes, the excited PS participates in a redox reaction with neighboring molecules by transferring a proton or an electron to form a radical cation or a radical anion, respectively. Such radicals may further react with oxygen to produce reactive oxygen species (ROS). In Type 2 processes, the triplet PS transfers its energy directly to molecular oxygen, to form singlet oxygen ($^1O_2$). Singlet oxygen reacts with a wide range of biological targets including DNA, RNA, proteins, and lipids. Rate constants for a large number of these reactions have been reported (Wilkinson et al. 1995).

Since energy transfer to yield $^1O_2$ usually competes with electron transfer, it is generally accepted that most PSs generate both $^1O_2$ and radicals. Energy transfer to O_2, however, is more rapid ($k \approx 1–3 \times 10^9$ M^{-1} s^{-1}) than electron transfer (e.g. to give $O_2^{\cdot-}$, estimated as $k \leq 1 \times 10^7$ M^{-1} s^{-1}) (Davies 2004), and chemically $^1O_2$ is more reactive than $O_2^{\cdot-}$. Therefore, singlet oxygen is considered the main damaging species in PDT. The relative contribution of Type 1 and Type 2 processes to the generation of reactive species will depend mainly on the chemical nature of the PS, the environment, and the concentration of oxygen.

Type 1 pathways frequently involve initial production of superoxide ($O_2^{\cdot-}$) by electron transfer from the triplet PS to molecular oxygen (monovalent reduction). Its lifetime in a biological environment has been estimated to be 30–40 μs, corresponding to a diffusion distance ~0.5 μm (Mikkelsen and Wardman 2003). Superoxide is not very reactive and cannot directly react with lipids and nucleic acids, or most amino acid residues in proteins. This low reactivity makes $O_2^{\cdot-}$-induced damage selective (Fridovich 1998). At pH values close to neutral, $O_2^{\cdot-}$ cannot cross membranes, except through anion channels (Korshunov and Imlay 2002; Lynch and Fridovich 1978), and its rate of spontaneous dismutation is so slow that it exists long enough to oxidize polyphenols, catecholamines, leukoflavines, and other small molecules (Fridovich 1998). Most importantly, $O_2^{\cdot-}$ can be involved in processes leading to the production of highly reactive species. First, dismutation of superoxide, accelerated in most organisms by the family of superoxide dismutases (SODs), produces hydrogen peroxide. Hydrogen peroxide is relatively stable, can cross membranes, and can diffuse away from its site of formation. Second, $O_2^{\cdot-}$ can directly interact with $[4Fe–4S]^{2+}$ clusters-containing proteins thus releasing 'free' iron (Imlay 2008; Liochev 1996), which then catalyzes the decomposition of H_2O_2 with the production of hydroxyl radical ($HO^{\cdot}$) (Fenton reaction). Hydroxyl radical can react indiscriminately with practically all biomolecules. Due to its extremely short half-life, however, it is assumed that only $HO^{\cdot}$ generated adjacent to biomolecules can cause damage (site specific). Third, superoxide can react at a diffusion-limited rate with nitric oxide ($NO^{\cdot}$) to produce peroxynitrite ($ONOO^-$), a powerful oxidant which can damage a wide variety of biomolecules including proteins, lipids, and nucleic acids (Ferrer-Sueta and Radi 2009; Groves 1999; Radi 2009).

Because of the high reactivity and short half-life of the damaging species produced by the photo-excited PSs, only molecules and structures that are in close proximity to the PS will be directly affected. For example, the half-life of singlet oxygen in biological systems is estimated to be less than 40 ns, which corresponds to a diffusion distance of no more than 20 nm (Moan 1990; Moan and Berg 1991). Therefore, the damage and type of response triggered by the activation of PSs will depend on their intracellular localization.

Zn(II) *N*-alkylpyridylporphyrin-based photosensitizers

A number of PSs are tetrapyrrole-based structures. These include porphyrins, chlorins, bacteriochlorins, benzoporphyrins, and phthalocyanines (Nyman and Hynninen 2004). The four nitrogen atoms of the tetrapyrrole macrocycle can chelate metal ions, which in turn modulates important photophysical parameters that determine the efficiency of a photosensitizer (Kee et al. 2008). Among the tetrapyrrole based PSs, Zn(II) *N*-alkylpyridylporphyrins (ZnPs) (Fig. 2) appeared as a promising group of highly efficient PSs (Benov et al. 2002). Tetrapyrrole structure offers almost unlimited possibilities for substitution, which allows design of molecules with varying physical and chemical parameters. Since interaction with oxygen and generation of reactive species is considered a key cell/tissue damaging factor, the longer the triplet excited state of the PS, the higher are the chances for such interactions. The triplet state lifetimes for the metal-free *N*-alkylpyridylporphyrins are in the range 1.16–0.17 ms and decrease

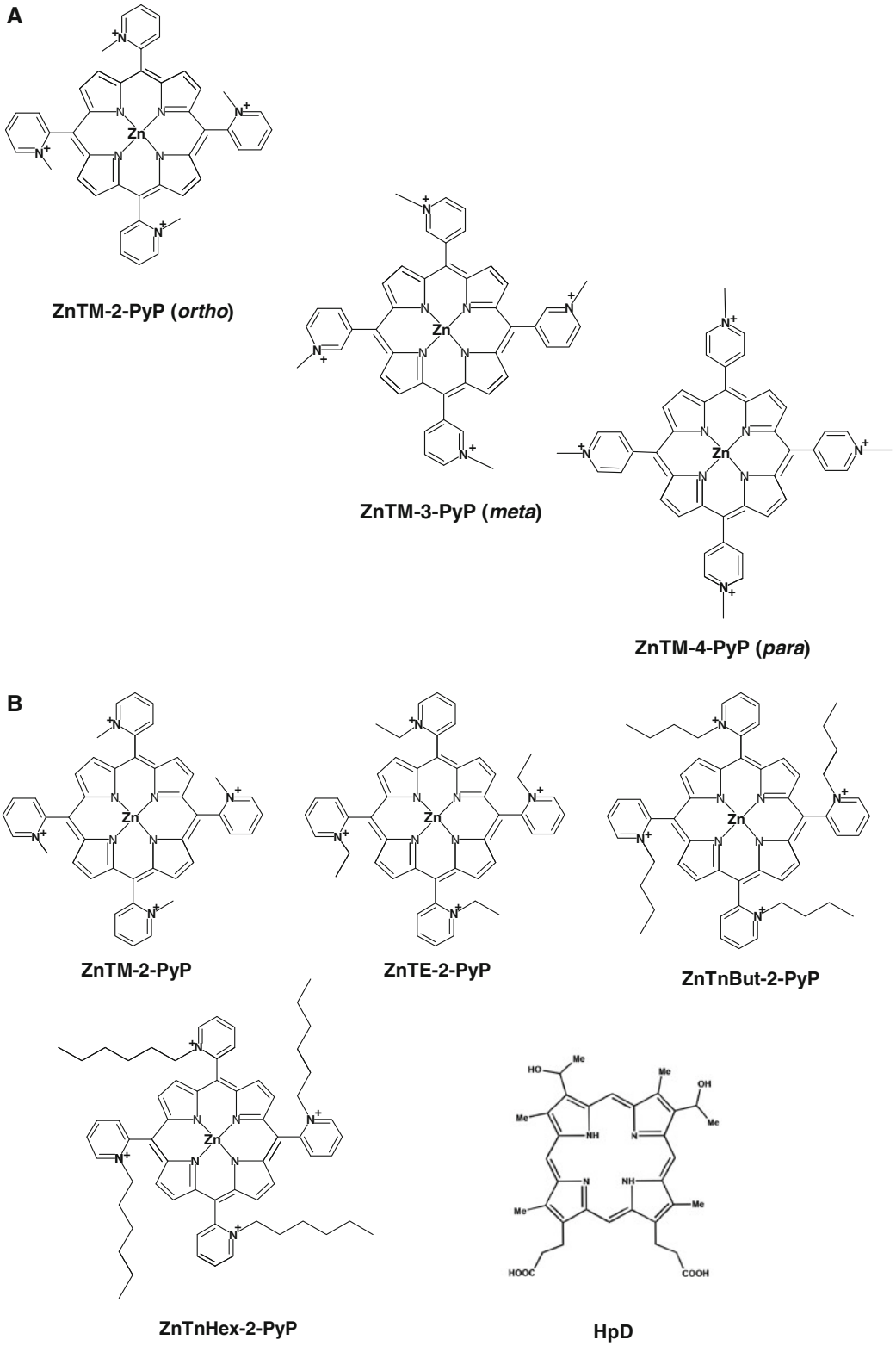

Fig. 2 Structures of Zn(II) *N*-alkylpyridyl porphyrins and hematoporphyrin D (HpD). A slightly modified composition, Photofrin, is used clinically as a photosensitizer. It is important to note that ZnPs are cationic while HpD is an anionic photosensitizer. Differences in charges determine their binding in vivo, and thus their sites of action and the types of biomolecules affected. **a** *ortho*, *meta*, and *para* Zn(II) *meso*-tetrakis(*N*-methylpyridinium-2, -3 and 4-yl)porphyrin, abbreviated as ZnTM-2-PyP (Charges are omitted throughout text for simplicity) (*ortho*), ZnTM-3-PyP (*meta*), and ZnTM-4-PyP (*para*). **b** Zn(II) *N*-alkylpyridylporphyrins, *ortho* series (methyl, ethyl, butyl and hexyl), and HpD monomer

along the series *ortho* > *meta* > *para* isomers (Kalyanasundaram 1983). Introduction of zinc increases the triplet lifetimes to 1.4 ms for ZnTM-2-PyP[1], and 2.0 ms for the *meta* (ZnTM-3-PyP) and *para* (ZnTM-4-PyP) isomers (Fig. 2a) (Kalyanasundaram 1983).

In addition to its intrinsic photophysical properties, the efficiency of a photosensitizer depends on its uptake and biodistribution, which is in turn controlled by the chemical character of the molecule. Two main features, the type and number of charges and the hydrophobicity (lipophilicity), determine the mode of entry and subcellular distribution of the photosensitizer (Juzeniene and Moan 2007). Appropriate combination of hydrophilicity and hydrophobicity is characteristic of some of the most potent PDT agents (Boyle and Dolphin 1996). Amphiphilicity often results from an asymmetric distribution of charged groups around the periphery of the macrocycle. The region of the porphyrin most distant from the charged groups then acts as a hydrophobic domain.

Hydrophobic PSs that possess two or fewer negative charges can diffuse across the plasma membrane and then relocate to other intracellular membranes. Such PSs also tend to show the greatest uptake into cells even when present at relatively low concentrations in the medium (Castano et al. 2004). More than two negative charges prevent free diffusion across the plasma membrane and such PSs are predominantly taken up by endocytosis (Boyle and Dolphin 1996; Castano et al. 2004). In general, hydrophobic PSs localize mainly in membranes, while hydrophilic PSs are confined to lysosomes (Boyle and Dolphin 1996; Juzeniene and Moan 2007). In turn, PSs bearing a net cationic charge were found predominantly in mitochondria, and those with net anionic character appear in lysosomes (Boyle and Dolphin 1996). Hydrophilic porphyrins with two anionic charges demonstrate a diffuse distribution in the cytoplasm (Boyle and Dolphin 1996).

Studies on the bioavailability of Mn porphyrins (Kos et al. 2009a, 2009b) have provided insights into the preparation ZnP analogs with targeted lipophilicity, without affecting the net positive charge of the molecule. Both *ortho* and *meta* isomers of Mn(III) *N*-alkylpyridylporphyrins have been characterized with respect to partition between n-octanol and water, P_{OW} (Kos et al. 2009a). The P_{OW} data demonstrated that we can enhance the lipophilicity by tenfold when we increase the *N*-alkyl chains by each additional carbon atom or move the *N*-alkyl groups from *ortho* onto *meta* pyridyl positions (Kos et al. 2009a, 2009b). Thus in the *ortho* series, the log P_{OW} is −7.86 for methyl, −5.11 for n-butyl, and −2.76 for n-hexyl porphyrin (Kos et al. 2009b). The relative changes in the lipophilicity, imposed by the changes in porphyrin periphery, should hold regardless of the type of the metal bound to the structure. Variations in the length of alkyl pyridyl chains were used to design a photosensitizer of desired lipophilicity. Progressive increase of the lipophilicity of *ortho* Zn *N*-alkylpyridylporphyrins as the alkyl chains were lengthened from methyl to hexyl, totaling five orders of magnitude, increased the accumulation of the PS in cancer cells (Fig. 3). This coincided with an increase of the photodynamic killing by ZnP analogs in the order: hexyl > butyl > methyl (Fig. 8). The potency of individual photosensitizers may also depend on the cell type (Morgan and Oseroff 2001). A separate set of experiments attempted to distinguish between PSs accumulated in the cytosol and PSs bound to membranes by separating cytosolic and membrane fractions by centrifugation (Kos et al. 2009a). Due to the low sensitivity of the method and the small quantity of material in the membrane fraction, no reliable data on the accumulation of PSs in membranes could be obtained, but accumulation of PSs in cytosolic fraction followed the pattern shown in Fig. 3.

A disadvantage of cationic photosensitizers is their considerable dark toxicity. For nonporphyrin-based PSs, this is related to the impairment of respiratory chain activity by uncoupling of electron transport and ATP synthesis (Morgan and Oseroff 2001). The toxicity of Mn-porphyrin analogs increases with the increase of their lipophilicity (Kos et al. 2009a). However, comparison of the members of the series of *ortho* Zn *N*-alkylpyridylporphyrins revealed no detectable dark toxicity in cultured mammalian cells over the concentration range used in our experiments (up to 25 μM). The marked difference between the manganese and zinc *N*-alkylpyridylporphyrin analogs implies that in addition to hydrophobicity, toxicity of Mn analogs also depends on their redox activity.

Proteins as photosensitizer targets

Compared to other classes of biomolecules, proteins can be considered primary targets for PS-derived reactive species, because they are highly abundant and rate constants for reactions with such species (mainly $^1O_2$) are often higher than with other potential targets (Davies 2003; Wilkinson et al. 1995). On the other hand, rate constants for the reaction of $^1O_2$ with different amino acid residues vary dramatically, which results in selective damage to particular amino acid side chains. Under physiological conditions, only Trp, His, Tyr, Met, and Cys react with $^1O_2$ at significant rates (Davies 2003). Photo-treatment of amino acids with ZnP photosensitizers under physiological

[1] ZnTalkyl-2,3,4-PyP^{5+} Zn(II) *meso*-tetrakis(*N*-alkylpyridinium-2 or 3-yl)porphyrin, alkyl being methyl (ZnTM-2-PyP, ZnTM-3-PyP, ZnTM-4-PyP), ethyl (ZnTE-2-PyP), n-butyl (ZnTnBu-2-PyP), and n-hexyl (ZnTnHex-2-PyP) 2, 3, and 4 relate to *ortho*, *meta*, and *para* isomers, respectively. Hematoporphyrin D, HpD.

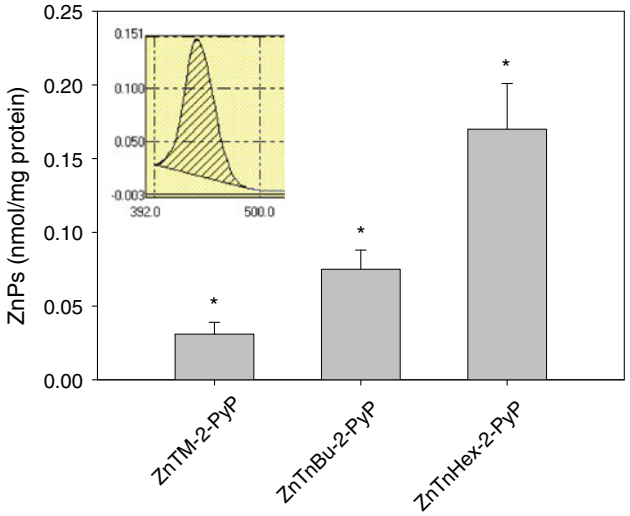

Fig. 3 Cellular accumulation of isomeric Zn *N*-alkylpyridylporphyrins. Accumulation of isomeric Zn *N*-alkylpyridylporphyrins in LS174T cells after 24 h of incubation with 5 μM ZnPs. After incubation, the cells were washed twice with PBS, resuspended to a final volume of 1.0 ml in PBS and disrupted by sonication. SDS was then added to a final concentration of 10%, samples were kept at 37°C for 4 h and centrifuged at 100,000×*g* for 1 h. Spectra of the clear supernatants were determined using a Shimadzu recording spectrophotometer and the areas under the peaks at Soret bands were calculated (*inset*). A standard curve was constructed by adding known concentrations of ZnPs to cell-free extracts prepared as described above. Data are presented as nmol of ZnP per mg of protein. *Bars* represent mean ± SE ($n = 3$). *Asterisks* indicate statistically significant differences among the groups, $p < 0.05$

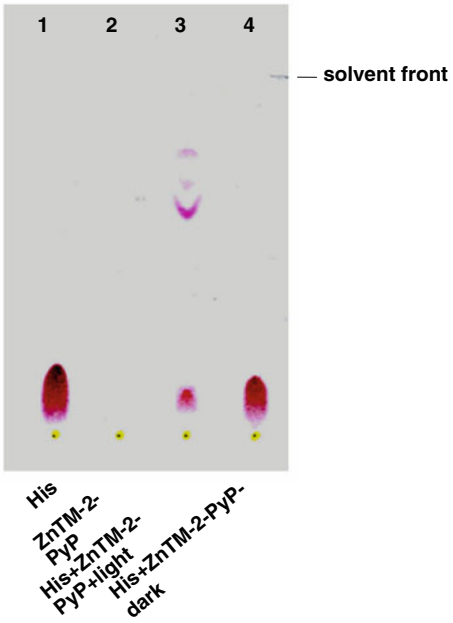

Fig. 4 Histidine modification after illumination with ZnPs. Histidine (10 mM) with or without ZnTM-2-PyP (2 μM) in phosphate buffered saline, pH 7.4 was illuminated or incubated in the dark for 30 min. Analysis using thin layer chromatography on silica gel; mobile phase was ethanol/water 1:1 (v/v) at room temperature. After drying, the chromatogram was sprayed with ninhydrin reagent and heated to reveal species with reactive alpha-amino groups. *Lanes*: (*1*) 10 mM histidine illuminated in the absence of ZnP, (*2*) 2 μM ZnTM-2-PyP, (*3*) 10 mM histidine illuminated in the presence of 2 μM ZnTM-2-PyP, (*4*) 10 mM histidine and 2 μM ZnTM-2-PyP incubated in the dark. The experiment was repeated three times with similar outcome. One representative thin layer chromatogram is shown

conditions has shown more rapid modification of histidine than any other amino acid, with generation of multiple products (Fig. 4). Considering $^1O_2$ as the main PDT protein damaging factor, it follows that modification of an individual protein will depend on the content and position of the vulnerable amino acid residues in the protein structure, and the ability of the PS to reach such vulnerable sites. Reactive species generated by the photo-activated PS can lead to various chemical modifications of the amino acid side chains, including carbonylation and formation of peroxides. As a consequence, affected proteins could undergo conformational changes, unfolding, fragmentation, and cross-linking. Such changes would ultimately result in a loss of function, including loss of enzyme catalytic activity.

Enzyme inactivation

Protein damage by photo-activated ZnPs is rather specific. This specificity is manifested by selective inactivation of cellular enzymes, and is dependent upon the ability of the photosensitizer to generate reactive species in close proximity to critical and sensitive amino acid residues.

Antioxidant enzymes

Both superoxide dismutase (SOD) and catalase are readily inactivated by $^1O_2$. The rate constants for the $^1O_2$-induced loss of activity have been established as 3.9×10^7 M^{-1} s^{-1} for SOD and 2.5×10^7 M^{-1} s^{-1} for catalase (Escobar et al. 1996). Indeed, significant loss of CuZnSOD, MnSOD, and catalase activities were reported for keratinocytes treated with Photofrin and illuminated (Luo et al. 2006). These enzymes were not inactivated, however, when human colon adenocarcinoma LS174T cells were treated with ZnTM-3-PyP and illuminated with visible light (Al-Mutairi et al. 2007b). Under the same conditions, glutathione reductase and glutathione peroxidase almost completely lost their activities during the illumination period, a process accompanied by a profound drop in GSH/GSSG ratio (Fig. 5) (Al-Mutairi et al. 2007b).

Evidence has also been presented for the modification of prosthetic groups within protein structures. Thus, exposure of catalase to $^1O_2$ has been shown to generate multiple conformers with more acidic isoelectric points as a result of the modification of the heme group (Lledias and Hansberg

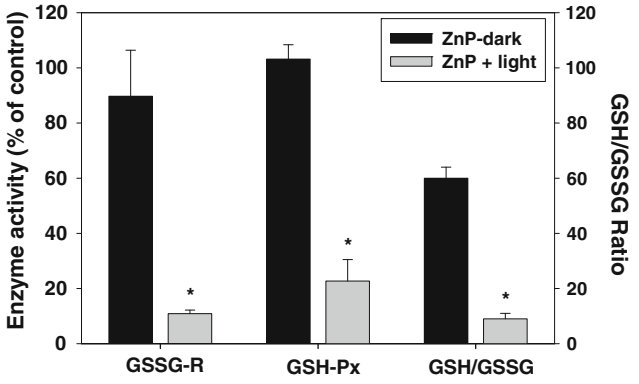

Fig. 5 Inactivation of antioxidant enzymes. LS174T cells (~80% confluent) loaded with 20 μM ZnTM-3-PyP in the dark were either illuminated for 30 min or kept in the dark (dark controls). Immediately after illumination, the medium was removed, the adherent cells were harvested, briefly washed with cold PBS, resuspended in the enzyme assay buffer and disrupted by sonication. Debris was removed by centrifugation and enzyme activities were determined. The GSH/GSSG ratio was measured using a Bioxytech GSH/GSSG-412 kit (Oxis International, Inc., Portland, OR, USA). To avoid GSH oxidation during sample handling, the adherent cells were scraped away from the plastic surface of the culture flask with a rubber policeman, rapidly centrifuged and briefly washed with 1.0 ml cold PBS. All procedures were performed in a cold room and centrifuge tubes were kept on ice. The cell pellet was used for the assay directly, without sonication. Mean ± SEM is presented ($n = 3$–5). *Asterisks* represent $p < 0.01$ compared to the non-treated controls. Adapted from reference (Al-Mutairi et al. 2007b)

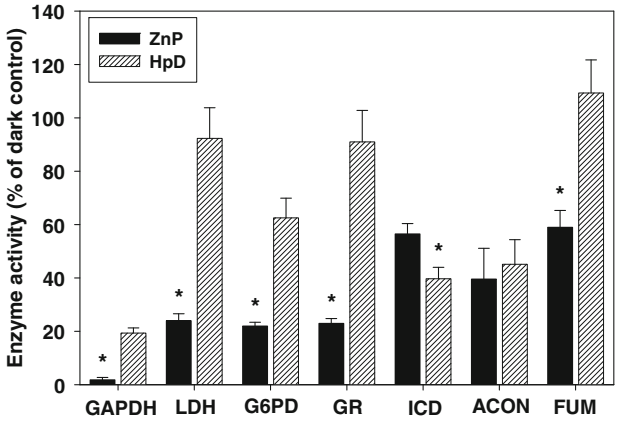

Fig. 6 Comparison between ZnTM-3-PyP and HpD. Sterile photosensitizers solutions were added to the growth medium to a final concentration of 20 μM. 24 h later the medium containing photosensitizers was removed, the cells were washed with PBS, resuspended in PBS, and illuminated. Immediately after the illumination, cells were harvested, briefly washed with cold PBS, resuspended in the respective enzyme assay buffers, and sonicated. Debris was removed by centrifugation and enzyme activities were assayed in the cell-free extracts. *GAPDH* glyceraldehyde-3-phosphate dehydrogenasem, *LDH* lactate dehydrogenase, *G6PD* glucose-6-phosphate dehydrogenase, *GR* glutathione reductase, *ICD* isocitrate dehydrogenase, *ACON* aconitase, *FUM* fumarase. Mean ± SE is presented ($n = 3$). *Asterisks* represent $p < 0.01$ compared to the non-treated controls. Adapted from Reference (Al-Mutairi et al. 2007a)

1999; Lledias et al. 1998). None of the ZnP-based PSs that we tested, however, induced changes in the catalase isoelectric point. This finding illustrates the importance of the protein–PS interaction and shows that the positioning of the two molecules is critical in determining PDT outcomes.

Metabolic enzymes

Increased glycolysis is a common feature of cancer that is observed consistently in many cancer types with various tissue origins (Pelicano et al. 2006). Together with glycolysis, the pentose phosphate pathway is important for tumor proliferation because of its role in supplying tumor cells with NADPH and ribose-5-phosphate for DNA and RNA synthesis (Boros et al. 1998). Therefore, inhibition of glycolysis and/or the pentose phosphate pathway in tumors is a way of suppressing cancer cell proliferation. Experiments with cancer cells loaded with ZnPs have shown that upon photo-activation these PSs inhibit important enzymes of the glycolytic and pentose phosphate pathways. Glyceradehyde-3-phosphate dehydrogenase, lactate dehydrogenase, and glucose-6-phosphate dehydrogenase appeared to be extremely sensitive to photo-inactivation by ZnTM-3-PyP (Al-Mutairi et al. 2007a).

A comparison of cells loaded with either cationic ZnTM-3-PyP or anionic Hematoporphyrin D (HpD) and illuminated, shows that these photosensitizers differ considerably in their ability to inactivate enzymes (Fig. 6). Except for aconitase, which was almost equally inactivated by both ZnTM-3-PyP and HpD, and isocitrate dehydrogenase (ICD), where slightly greater inactivation was observed with HpD, enzyme photoinactivation caused by ZnTM-3-PyP was much greater than the photoinactivation induced by HpD. Lactate dehydrogenase (LDH), glucose-6-phosphate dehydrogenase (G6PD), and glyceraldehyde-3-phosphate dehydrogenase (GAPDH) activities were dramatically decreased in the ZnTM-3-PyP-loaded cells, but were not inactivated in the HpD-treated cells. This shows that protein damage is rather specific and depends on both the properties of proteins, structure and shape, and photosensitizer. These factors determine the proximity of the PS molecule to a target, and hence, which particular proteins will be affected and how much damage will be done.

Mitochondrial proteins

There has been a growing awareness of the role of mitochondria in numerous disease processes and development of drugs targeting mitochondria is an area of increasing importance. As noted earlier, positively charged photosensitizers tend to accumulate in the mitochondria, driven by membrane potential gradients. In addition to the number

of charges, mitochondrial accumulation of cationic PSs also depends on their lipophilicity (Castano et al. 2004; Dummin et al. 1997). For cationic Zn phthalocyanines, it was demonstrated that the more lipophilic members entered mitochondria more readily than less lipophilic molecules, confirming that proper targeting requires a suitable combination of charge and hydrophobic characteristics (Morgan and Oseroff 2001). Such data are in agreement with the recent trends in the design of mitochondrially targeted drugs which possess positive charge and a lipophilic component (Murphy and Smith 2007).

The reason for mitochondrial localization of positively charged PSs lies in the electrical polarization of the inner mitochondrial membrane. Proton pumping by respiratory chain complexes makes the matrix negatively charged relative to the intermembrane space. The combination of a membrane potential and a pH gradient provides the driving force for the selective uptake of positively charged PSs (Morgan and Oseroff 2001). As positively charged PS molecules accumulate in the matrix, the negative potential across the membrane drops. High levels of cationic PSs may eventually cause marked depolarization. In turn, the driving force for the PS accumulation is lost, which leads to PS redistribution to other cellular sites (Morgan and Oseroff 2001).

The reported photo-damage of mitochondrial components and impairment of mitochondrial functions provides evidence for the mitochondrial localization of PSs. Photo-induced decrease in the activity of mitochondrial enzymes (Hilf et al. 1984), ultrastructural changes (Coppola et al. 1980), and inhibition of membrane transport (Atlante et al. 1989), ATP production (Hilf 2007), and electron transport (Salet and Moreno 1995) have been reported (reviewed in detail by (Morgan and Oseroff 2001).

In vivo experiments showed that a cationic Mn(III) analog of Zn *N*-ethylpyridylporphyrin, MnTE-2-PyP, enters mitochondria (Spasojevic et al. 2007). Preliminary studies indicate that the cationic and lipophilic hexyl analog, MnTnHex-2-PyP, accumulates in mitochondria at a higher level than ethyl porphyrin, MnTE-2-PyP (Batinic-Haberle et al. 2010b). Lengthening of the alkyl chains should affect the mitochondrial localization of the modified porphyrins in a similar manner, regardless of the metal associated with the porphyrin. Given high levels of endogenous reductants such as ascorbate and glutathione, Mn porphyrins would be reduced in vivo and would probably accumulate within cells in a reduced state (Batinic-Haberle et al. 1998; Batinic-Haberle et al. 2010a; Kos et al. 2009a). Reduced tetracationic MnPs bear one less charge and are therefore significantly more lipophilic; their physical properties thus closely resemble tetracationic ZnPs. Given this strong similarity, it can be predicted with confidence that ZnTnHex-2-PyP would accumulate in mitochondria to a level similar to that found for MnTnHex-2-PyP^{5+}/MnTnHex-2-PyP^{4+}, and to a much higher level than that for the methyl analog. Further experimental work is needed to accurately measure accumulation of ZnPs in mitochondria and determine whether there is indeed marked selectivity for this organelle compared to other intracellular targets. As noted above, inactivation of mitochondrial enzymes can be used to assess mitochondrial photo-damage. Given the very short range of most photo-generated reactive species, the inactivation of Krebs cycle enzymes (Figs. 6, 7) (Al-Mutairi et al. 2007a) by a Zn methyl porphyrin, ZnTM-3-PyP, strongly suggests that the photosensitizer reaches mitochondria. However, since initial photo-damage can lead to redistribution of the PS during irradiation (Boyle and Dolphin 1996), it is difficult to determine if a PS specifically targets all those molecules that were subsequently found to be photo-damaged.

The short diffusion distance of $^1O_2$ allows identification of the cellular binding sites of photosensitizers, since only molecules in close proximity are damaged. This is well

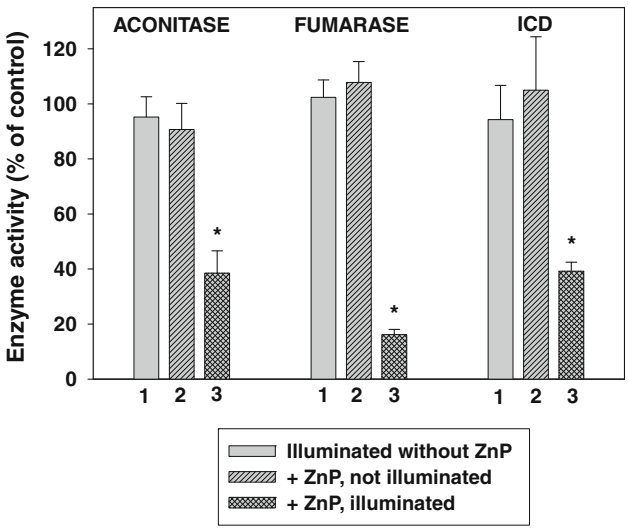

Fig. 7 Inactivation of mitochondrial enzymes in cancer cells loaded with ZnTM-3-PyP. Human colon adenocarcinoma LS174T cells were grown in minimal essential medium supplemented with 10% fetal bovine serum, 1.2% L-glutamine, 1.2% MEM nonessential amino acids, and 1.2% penicillin/streptomycin. Sterile solutions of the photosensitizers were added to the growth medium to a final concentration of 20 μM, and 24 h later the medium containing ZnPs was removed. The cells were washed with PBS, and then illuminated in PBS for 30 min. Activities of aconitase, fumarase, and isocitrate dehydrogenase (ICD) were determined as units per mg of protein immediately after the end of the illumination or dark incubation. Data for other ZnPs were obtained in a similar way. *Bars*: *1* illuminated in the absence of ZnP, *2* loaded with ZnP, but not illuminated, *3* loaded with ZnPs and illuminated. Experiments were repeated at least three times with 3–5 replicates. The means ± SE are presented. Statistical analysis was performed using ANOVA. *Asterisks* represent $p < 0.01$ compared to the non-treated controls. Adapted from Ref. (Al-Mutairi et al. 2007a)

illustrated by the differential inactivation of mitochondrial enzymes by photo-activated ZnPs. In cancer cells loaded with ZnTM-3-PyP ~90% of fumarase, ~60% of aconitase, and ~50% of isocitrate dehydrogenase activities were lost within 30 min of illumination (Fig. 7) (Al-Mutairi et al. 2007a).

It is clear that inactivation of metabolic cytosolic and mitochondrial enzymes compromises a cell's capacity to generate NADH and therefore energy, as well as to maintain its redox status via NADPH production. All those effects lead to the failure of the photo-damaged cell to reduce 3-(4,5-dimethylthiazol-2-yl)-2,5-diphenyltetrazolium bromide (MTT) to blue formazan (Al-Mutairi et al. 2007b). The MTT test is commonly used to assess cell viability and proliferation, but its reduction reflects the availability of reducing equivalents and thus the metabolic state of the cells (Berridge et al. 2005; Berridge and Tan 1993).

Based on the analogies between Zn and Mn porphyrins noted above, ZnTnHex-2-PyP is expected to be ~5 and ~2.5 orders of magnitude more lipophilic than methyl, ZnTM-2-PyP and butyl, ZnTnBu-2-PyP, respectively. ZnTM-2-PyP, ZnTnBu-2-PyP, and ZnTnHex-2-PyP were tested with respect to their ability to inhibit cellular reduction of MTT in a photo-dependent manner, as a consequence of their inflicting damage upon cellular metabolism (Fig. 8). The most lipophilic, ZnTnHex-2-PyP, showed the highest potency.

Even when different photosensitizers target the same organelles and accumulate to the same extent, their effectiveness can vary considerably (Morgan and Oseroff 2001). It has been reported, for example, that hematoporphyrin is more efficient photosensitizer than protoporphyrin IX even though they both accumulate to the same level in mitochondria. Since equivalent amounts of singlet oxygen are produced by hematoporphyrin and protoporphyrin IX in their monomeric forms, the greater efficiency of hematoporphyrin was attributed to its enhanced ability to bind to proteins in the mitochondrial membrane (Morgan and Oseroff 2001). Compared to cationic ZnPs, the anionic HpD, which is lipophilic and localizes in plasma membrane, mitochondria, nuclear membrane and endoplasmic reticulum (Juzeniene and Moan 2007), was much less effective in inhibiting MTT reduction (Fig. 8). Since MTT reduction depends on metabolic activity, it can be concluded that ZnPs bind to metabolic enzymes with greater efficiency than HpD. Differences in efficacy between cationic ZnPs and anionic HpD can be at least in part ascribed to different charges they bear at the periphery: four positive symmetrically distributed charges of ZnPs versus two negative asymmetrically distributed charges with HpD.

Elongation of the aliphatic chains attached to the pyridyl nitrogen does not appear to appreciably affect the

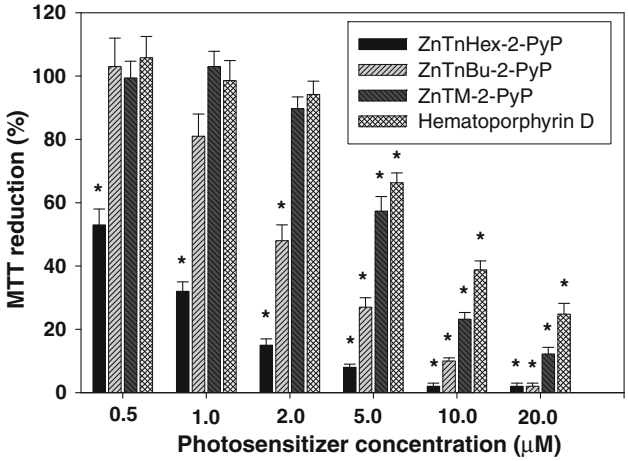

Fig. 8 Photodynamic suppression of cell metabolism. MTT reduction after illumination of LS174T cancer cells loaded with hematoporphyrin D or ZnP photosensitizers. Three ZnPs with vastly different hydrophobicity were used. Hexyl porphyrin, ZnTnHex-2-PyP is ~2.5 log units more lipophilic than butyl, ZnTnBu-2-PyP, and ~5 log units more lipophilic than methyl analog, ZnTM-2-PyP. Experimental protocol was as previously described for ZnTM-3-PyP (Al-Mutairi et al. 2007a). Sterile solutions of the photosensitizer were added to the growth medium and 24 h later the medium containing ZnPs was removed, the cells were washed with PBS, resuspended in PBS, and illuminated. After illumination, PBS was replaced with 1.0 ml of medium to which 50 μl of 5 mg/ml MTT solution was added. After 3 h of incubation in a CO_2 incubator, 0.5 ml of 10% SDS in 10 mM HCl were added and the plates were incubated overnight. The solubilized product was assayed at 560 nm, and the absorbance at 650 nm was used as a background. Parallel dark controls were run for each compound. None of the photosensitizers affected the reduction of MTT in the dark. Experiments were repeated three times with 3–5 replicates. Means ± SE are presented. *Asterisks* represent $p < 0.01$ compared to the non-treated controls

photophysical properties of the PSs, since in a cell-free system both butyl and hexyl derivatives demonstrated very similar photo-cross-linking of purified samples of lactate dehydrogenase, a globular hydrophilic cytosolic protein dissolved in physiological buffered saline solution (Fig. 9). Thus, the increased cellular PS efficacy of longer alkyl chain-substituted ZnPs principally reflects changes in cellular uptake and intracellular distribution and is a consequence of their increased lipophilicity and ability to bind particular proteins.

Structural changes

Enzyme inactivation can result from the modification of essential amino acid residues and relatively small alterations in the protein structure. Apart from the loss of catalytic activity, such changes may not lead to changes in the protein molecule that could be recognizable by common analytical techniques. Intense generation of ROS by photoactivated PSs, however, can cause profound damage to

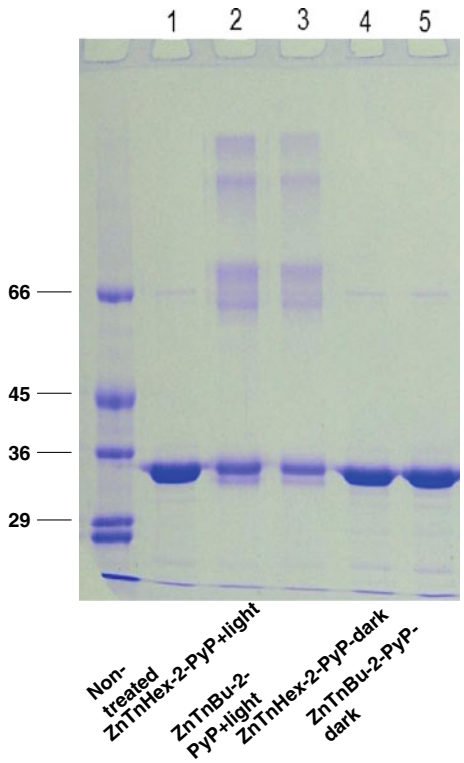

Fig. 9 Cross-linking of pure lactate dehydrogenase. Purified chicken muscle lactate dehydrogenase (LDH) (20 mg/ml in PBS, pH 7.4) was illuminated for 30 min in the presence of 2 μM ZnPs. Dark controls, containing the same concentration of ZnPs and controls illuminated in the absence of sensitizer were run in parallel. After illumination, the samples were subjected to SDS-PAGE analysis following solubilization by heating with sample buffer including 5% (v/v) 2-mercaptoethanol (7 min, 37°C). Protein loading was 10 μg/lane. *Lanes*: (*1*) non-treated, (*2*) illuminated in the presence of ZnTnHex-2-PyP, (*3*) illuminated in the presence of ZnTnBu-2-PyP, (*4*) ZnTnHex-2-PyP—dark control, (*5*) ZnTnBu-2-PyP—dark control. Molecular weight standards are also shown. For data regarding ZnTM PyP see (Al-Mutairi et al. 2007a). One representative electrophoretic separation is shown. The experiment was repeated five times with similar results

protein molecules, manifested as fragmentation and aggregation. Fragmentation seems to be encountered relatively rarely (Davies 2003). Lysozyme, exposed to photo-activated lumiflavin has been reported to undergo fragmentation, but the exact reactive species and chemical reactions involved are not known (Gomyo and Fujimaki 1970). In contrast, the PS-induced formation of high-molecular weight protein aggregates is well documented (Davies 2004, 2005; Verweij et al. 1981). Aggregation seems to be mediated by radical–radical reactions of Tyr-derived phenoxyl radicals to give di-tyrosine (Spikes et al. 1999), inter-molecular disulfide bond formation (Truscott and Augusteyn 1977), and eventually through His–His and His–Lys crosslinks (Davies 2003).

Increasing the hydrophobicity of ZnPs from methyl to hexyl porphyrins had negligible effects on PS-mediated intermolecular cross-linking of pure globular proteins (illustrated by the photo-dependent aggregation of lactate dehydrogenase by ZnTnBu-2-PyP and ZnTnHex-2-PyP, Fig. 9). However, in an intact cell system, the differences in their lipophilicities greatly influenced the PS-mediated ability to affect cell metabolism, i.e. MTT reduction (see above, Fig. 8).

Membrane proteins

Membrane damage is considered a major cause of PDT-induced cell death and manifested by chemical modifications of lipids and protein cross-linking and aggregation. Thus, together with lipids, membrane proteins are sensitive PDT targets (Juzeniene et al. 2006). Protein damage is probably the reason why cells in S phase are more sensitive to PDT than cells in G_1 and G_2 phases (Juzeniene et al. 2006). Increase in membrane permeability is one of the first events triggered by illumination in the presence of ZnP. In cultured human colon adenocarcinoma LS174T cells preloaded with 20 μM ZnTM-3-PyP, leakage of ATP takes place during the illumination period (Fig. 10) (Al-Mutairi et al. 2006), followed by increased permeability towards larger molecules (Al-Mutairi et al. 2007b). The leakage of ATP along with inactivation of metabolic enzymes is among the reasons for rapid depletion of ATP in photo-treated tumor cells, leading eventually to cell death.

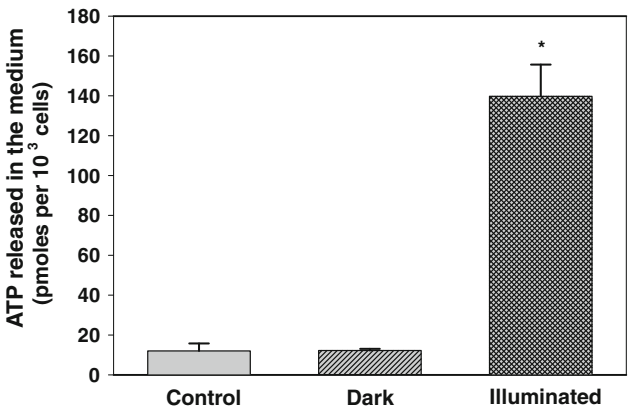

Fig. 10 ATP leakage from the photo-treated cells. The leakage of ATP from LS174T cells was determined for controls, 20 μM ZnTM-3-PyP-treated in the dark, and 20 μM ZnTM-3-PyP-illuminated groups. Immediately after the illumination, 50 μl samples of the medium were transferred into eppendorf tubes and centrifuged for 3 min at 4°C. Aliquots (25 μl) of the supernatant were taken and ATP was measured with an ATP Bioluminescent Assay Kit (Sigma) according to the manufacturer's instructions. The mean ± SEM is presented. Experiments were repeated three times with three replicates. $*p < 0.005$ compared to control. Adapted from Reference (Al-Mutairi et al. 2006)

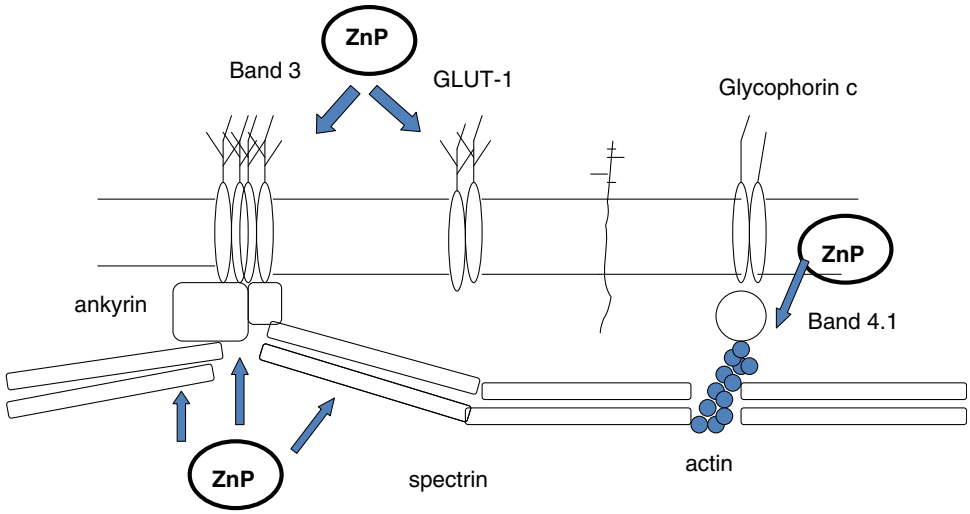

Fig. 11 Schematic presentation of human red blood cell membrane proteins targeted by ZnP photosensitizers. *Arrows* indicate sensitive sites in isolated membranes. Extrinsic structural proteins showed rapid and extensive cross-linking under the experimental conditions chosen (see Fig. 12)

Photo-induced ATP loss may result directly from the general membrane damage, or activation of channels such as those reported to mediate ATP release in response to mechanical or osmotic stress, or hypoxia (Dutta et al. 2004; Hazama et al. 2000; Sabirov et al. 2001).

As with cytosolic and mitochondrial proteins, membrane proteins differ widely with respect to their susceptibility to modification by excited PSs. PS-mediated membrane protein damage is illustrated using the isolated erythrocyte membrane as a model system and the most lipophilic ZnTnHex-2-PyP, which exerted the highest effect on cancer cell metabolism. Major extrinsic membrane proteins forming the membrane cytoskeleton and its junctional complexes, including spectrin, actin, band 3 (anion exchanger AE1), band 4.1, and ankyrin (Fig. 11), are rapidly and extensively cross-linked as exemplified here with the loss of spectrin bands when erythrocyte membranes are photo-treated with 2 μM ZnTnHex-2-PyP (Fig. 12). Samples were subjected to treatment with 2-mercaptoethanol for SDS-PAGE analysis, and so the observed cross-linking was not caused by the formation of disulfide bonds. While the major integral membrane protein, an anion exchanger (band 3, AE1), much of which associates with the cytoskeleton (Low 1986), is a sensitive target, the glucose transporter GLUT-1 (a hydrophobic integral membrane protein believed to be an obligate dimer) exhibits slower aggregation (not shown).

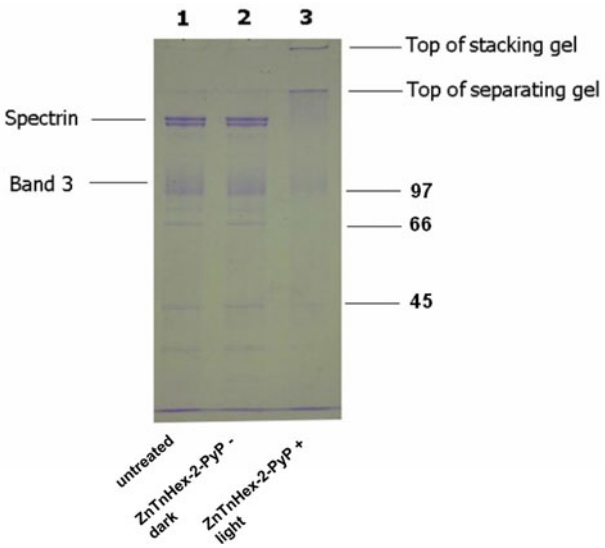

Fig. 12 Cross-linking of membrane proteins. Isolated human erythrocyte membranes were illuminated with or without ZnTnHex-2-PyP. Dark controls were run in parallel. Immediately after illumination, membranes were solubilized in the dark followed by SDS-PAGE analysis (4% stacking gel, 10% separating gel). Protein loading was 15 μg/lane and migration of molecular weight standards (97, 66 and 45 kDa) is indicated. *Lanes*: (*1*) untreated membranes, (*2*) treated with 2 μM ZnTnHex-2-PyP in the dark, (*3*) treated with 2 μM ZnTnHex-2-PyP and illuminated with visible light for 20 min. The dark control confirms that photo-cross-linking did not occur during the analytical procedures. Treatment with Hematoporphyrin D (Photofrin) at an identical concentration resulted in no detectable cross-linking under these conditions. One representative electrophoretic separation is shown. The experiment was repeated more than six times with similar results

Concluding remarks

PDT is advantageous compared to the traditional treatments of cancer and other diseases because of the selectivity, non-invasiveness and high efficiency coupled with a lack of serious side effects and drug resistance. These advantages have stimulated the search for better and more efficient photosensitizers and specific, well-defined cellular targets. Because of their diverse and essential functions and abundance, proteins are regarded as key targets for PDT. Designing PSs that aim at specific proteins is an important avenue for achieving high selectivity in PDT. Experience based on Zn(II) *N*-alkylpyridylporphyrins and

their photo-inactive Mn(III) analogs shows that proper selection of the photosensitizer core and variations in the distribution of the functional groups on its periphery, could eventually lead to the design of highly selective photosensitizers, capable of targeting not only particular cellular compartments or membrane structures, but even specific polypeptides.

Acknowledgments LB and JC are grateful for the financial support by grants MB 07/04, MB 03/07, and YM 02/08 from Kuwait University and to Research Core Facility (GM01/01 and GM01/05). IBH acknowledges the support from NIH U19 AI67798, Wallace H Coulter Translational Partners Grant Program, and NIH-IR21-ESO/3682. The authors are grateful to Dr. Irwin Fridovich for his guidance, ideas and continuous help.

References

Al-Mutairi DA, Craik JD, Batinic-Haberle I, Benov LT (2006) Photosensitizing action of isomeric zinc *N*-methylpyridyl porphyrins in human carcinoma cells. Free Radic Res 40:477–483

Al-Mutairi DA, Craik JD, Batinic-Haberle I, Benov LT (2007a) Inactivation of metabolic enzymes by photo-treatment with zinc meta *N*-methylpyridylporphyrin. Biochim Biophys Acta 1770:1520–1527

Al-Mutairi DA, Craik JD, Batinic-Haberle I, Benov LT (2007b) Induction of oxidative cell damage by photo-treatment with zinc *N*-methylpyridylporphyrin. Free Radic Res 41:89–96

Atlante A, Passarella S, Quagliariello E, Moreno G, Salet C (1989) Haematoporphyrin derivative (Photofrin II) photosensitization of isolated mitochondria: inhibition of ADP/ATP translocator. J Photochem Photobiol B 4:35–46

Batinic-Haberle I, Benov L, Spasojevic I, Fridovich I (1998) The ortho effect makes manganese(III) meso-tetrakis(*N*-methylpyridinium-2-yl)porphyrin a powerful and potentially useful superoxide dismutase mimic. J Biol Chem 273:24521–24528

Batinic-Haberle I, Reboucas J, Benov L, Spasojevic I (2010a) Chemistry, biology and medical effects of water-soluble porphyrins. In: Kadish K, Smith K, Guillard R (eds) Handbook of porphyrin science, vol XI, World Scientific (in press)

Batinic-Haberle I, Spasojevic I, Piganelli JD, Reboucas JS, Dewhirst MW, Vujaskovic Z, Warner DS, St Clair DK (2010b) The remarkable potency of Mn-porphyrins in treating oxidative stress injuries arises from their differential tissue and subcellular distribution and interaction with redox-based transcription factors. In: 6th International conference on porphyrins and phthalocyanines, ICPP-6, New Mexico

Benov L, Batinic-Haberle I, Spasojevic I, Fridovich I (2002) Isomeric *N*-alkylpyridylporphyrins and their Zn(II) complexes: inactive as SOD mimics but powerful photosensitizers. Arch Biochem Biophys 402:159–165

Berridge MV, Tan AS (1993) Characterization of the cellular reduction of 3-(4, 5-dimethylthiazol-2-yl)-2, 5-diphenyltetrazolium bromide (MTT): subcellular localization, substrate dependence, and involvement of mitochondrial electron transport in MTT reduction. Arch Biochem Biophys 303:474–482

Berridge MV, Herst PM, Tan AS (2005) Tetrazolium dyes as tools in cell biology: new insights into their cellular reduction. Biotechnol Annu Rev 11:127–152

Boros LG, Lee PW, Brandes JL, Cascante M, Muscarella P, Schirmer WJ, Melvin WS, Ellison EC (1998) Nonoxidative pentose phosphate pathways and their direct role in ribose synthesis in tumors: is cancer a disease of cellular glucose metabolism? Med Hypotheses 50:55–59

Boyle RW, Dolphin D (1996) Structure and biodistribution relationships of photodynamic sensitizers. Photochem Photobiol 64:469–485

Castano AP, Demidova TN, Hamblin MR (2004) Mechanisms in photodynamic therapy: Part one-Photosensitizers, photochemistry and cellular localization. Photodiagnosis Photodyn Ther 1:279–293

Castano AP, Mroz P, Hamblin MR (2006) Photodynamic therapy and anti-tumour immunity. Nat Rev Cancer 6:535–545

Chen B, Pogue BW, Hoopes PJ, Hasan T (2006) Vascular and cellular targeting for photodynamic therapy. Crit Rev Eukaryot Gene Expr 16:279–305

Coppola A, Viggiani E, Salzarulo L, Rasile G (1980) Ultrastructural changes in lymphoma cells treated with hematoporphyrin and light. Am J Pathol 99:175–192

Davies MJ (2003) Singlet oxygen-mediated damage to proteins and its consequences. Biochem Biophys Res Commun 305:761–770

Davies MJ (2004) Reactive species formed on proteins exposed to singlet oxygen. Photochem Photobiol Sci 3:17–25

Davies MJ (2005) The oxidative environment and protein damage. Biochim Biophys Acta 1703:93–109

Donnelly RF, McCarron PA, Tunney MM (2008) Antifungal photodynamic therapy. Microbiol Res 163:1–12

Dummin H, Cernay T, Zimmermann HW (1997) Selective photosensitization of mitochondria in HeLa cells by cationic Zn(II)phthalocyanines with lipophilic side-chains. J Photochem Photobiol B 37:219–229

Dutta AK, Sabirov RZ, Uramoto H, Okada Y (2004) Role of ATP-conductive anion channel in ATP release from neonatal rat cardiomyocytes in ischaemic or hypoxic conditions. J Physiol 559:799–812

Escobar JA, Rubio MA, Lissi EA (1996) SOD and catalase inactivation by singlet oxygen and peroxyl radicals. Free Radic Biol Med 20:285–290

Ferrer-Sueta G, Radi R (2009) Chemical biology of peroxynitrite: kinetics, diffusion, and radicals. ACS Chem Biol 4:161–177

Foote CS (1991) Definition of type I and type II photosensitized oxidation. Photochem Photobiol 54:659

Fridovich I (1998) Oxygen toxicity: a radical explanation. J Exp Biol 201:1203–1209

Gomyo T, Fujimaki M (1970) Studies on changes in protein by dye sensitized photooxidation. Part 3: On the photodecomposition products of lysozyme. Agric Biol Chem 34:302–309

Groves JT (1999) Peroxynitrite: reactive, invasive and enigmatic. Curr Opin Chem Biol 3:226–235

Hazama A, Fan HT, Abdullaev I, Maeno E, Tanaka S, Ando-Akatsuka Y, Okada Y (2000) Swelling-activated, cystic fibrosis transmembrane conductance regulator-augmented ATP release and Cl-conductances in murine C127 cells. J Physiol 1:1–11

Hilf R (2007) Mitochondria are targets of photodynamic therapy. J Bioenerg Biomembr 39:85–89

Hilf R, Warne NW, Smail DB, Gibson SL (1984) Photodynamic inactivation of selected intracellular enzymes by hematoporphyrin derivative and their relationship to tumor cell viability in vitro. Cancer Lett 24:165–172

Imlay JA (2008) Cellular defenses against superoxide and hydrogen peroxide. Annu Rev Biochem 77:755–776

Juarranz A, Jaaen P, Sanz-Rodriguez F, Cuevas J, Gonzalez S (2008) Photodynamic therapy of cancer. Basic principles and applications. Clin Transl Oncol 10:148–154

Juzeniene A, Moan J (2007) The history of PDT in Norway. Part one: Identification of basic mechanisms of general PDT. Photodiagnosis Photodyn Ther 4:3–11

Juzeniene A, Nielsen KP, Moan J (2006) Biophysical aspects of photodynamic therapy. J Environ Pathol Toxicol Oncol 25:7–28

Kalyanasundaram K (1983) Photochemistry of water-soluble porphyrins: comparative study of Isomeric tetrapyridyl- and tetrakis(*N*-Methylpyridiniumyl)porphyrins. Inorg Chem 23:2453–2459

Kee HL, Bhaumik J, Diers JR, Mroz P, Hamblin MR, Bocian DF, Lindsey JS, Holten D (2008) Photophysical characterization of imidazolium-substituted Pd(II), In(III), and Zn(II) porphyrins as photosensitizers for photodynamic therapy. J Photochem Photobiol A Chem 200:346–355

Korshunov SS, Imlay JA (2002) A potential role for periplasmic superoxide dismutase in blocking the penetration of external superoxide into the cytosol of Gram-negative bacteria. Mol Microbiol 43:95–106

Kos I, Benov L, Spasojevic I, Reboucas JS, Batinic-Haberle I (2009a) High lipophilicity of meta Mn(III) *N*-alkylpyridylporphyrin-based superoxide dismutase mimics compensates for their lower antioxidant potency and makes them as effective as ortho analogues in protecting superoxide dismutase-deficient *Escherichia coli*. J Med Chem 52:7868–7872

Kos I, Reboucas JS, DeFreitas-Silva G, Salvemini D, Vujaskovic Z, Dewhirst MW, Spasojevic I, Batinic-Haberle I (2009b) Lipophilicity of potent porphyrin-based antioxidants: comparison of ortho and meta isomers of Mn(III) *N*-alkylpyridylporphyrins. Free Radic Biol Med 47:72–78

Liochev SI (1996) The role of iron-sulfur clusters in in vivo hydroxyl radical production. Free Radic Res 25:369–384

Lledias F, Hansberg W (1999) Oxidation of human catalase by singlet oxygen in myeloid leukemia cells. Photochem Photobiol 70:887–892

Lledias F, Rangel P, Hansberg W (1998) Oxidation of catalase by singlet oxygen. J Biol Chem 273:10630–10637

Low PS (1986) Structure and function of the cytoplasmic domain of band 3: center of erythrocyte membrane-peripheral protein interactions. Biochim Biophys Acta 864:145–167

Luo J, Li L, Zhang Y, Spitz DR, Buettner GR, Oberley LW, Domann FE (2006) Inactivation of primary antioxidant enzymes in mouse keratinocytes by photodynamically generated singlet oxygen. Antioxid Redox Signal 8:1307–1314

Lynch RE, Fridovich I (1978) Permeation of the erythrocyte stroma by superoxide radical. J Biol Chem 253:4697–4699

Mikkelsen RB, Wardman P (2003) Biological chemistry of reactive oxygen and nitrogen and radiation-induced signal transduction mechanisms. Oncogene 22:5734–5754

Moan J (1990) On the diffusion length of singlet oxygen in cells and tissues. J Photochem Photobiol B 6:343–344

Moan J, Berg K (1991) The photodegradation of porphyrins in cells can be used to estimate the lifetime of singlet oxygen. Photochem Photobiol 53:549–553

Morgan J, Oseroff AR (2001) Mitochondria-based photodynamic anti-cancer therapy. Adv Drug Deliv Rev 49:71–86

Murphy MP, Smith RAJ (2007) Targeting antioxidants to mitochondria by conjugation to lipophilic cations. Annu Rev Pharmacol Toxicol 47:629–656

Nyman ES, Hynninen PH (2004) Research advances in the use of tetrapyrrolic photosensitizers for photodynamic therapy. J Photochem Photobiol B 73:1–28

Pelicano H, Martin DS, Xu RH, Huang P (2006) Glycolysis inhibition for anticancer treatment. Oncogene 25:4633–4646

Radi R (2009) Peroxynitrite and reactive nitrogen species: the contribution of ABB in two decades of research. Arch Biochem Biophys 484:111–113

Robertson CA, Evans DH, Abrahamse H (2009) Photodynamic therapy (PDT): a short review on cellular mechanisms and cancer research applications for PDT. J Photochem Photobiol B 96:1–8

Sabirov RZ, Dutta AK, Okada Y (2001) Volume-dependent ATP-conductive large-conductance anion channel as a pathway for swelling-induced ATP release. J Gen Physiol 118:251–266

Salet C, Moreno G (1995) Photodynamic action increases leakage of the mitochondrial electron transport chain. Int J Radiat Biol 67:477–480

Silva JN, Filipe P, Morliere P, Maziere J-C, Freitas JP, Gomes MM, Santus R (2008) Photodynamic therapy: dermatology and ophthalmology as main fields of current applications in clinic. Biomed Mater Eng 18:319–327

Spasojevic I, Chen Y, Noel TJ, Yu Y, Cole MP, Zhang L, Zhao Y, St. Clair DK, Batinic-Haberle I (2007) Mn porphyrin-based superoxide dismutase (SOD) mimic, MnIIITE-2-PyP5+ , targets mouse heart mitochondria. Free Radic Biol Med 42:1193–1200

Spikes JD, Shen H-R, Kopeckova P, Kopecek J (1999) Photodynamic crosslinking of proteins. III. Kinetics of the FMN- and rose bengal-sensitized photooxidation and intermolecular crosslinking of model tyrosine-containing *N*-(2-hydroxypropyl)methacrylamide copolymers. Photochem Photobiol 70:130–137

Taub AF (2007) Photodynamic therapy: other uses. Dermatol Clin 25:101–109

Truscott RJW, Augusteyn RC (1977) Oxidative changes in human lens proteins during senile nuclear cataract formation. Biochim Biophys Acta 492:43–52

Verweij H, Dubbelman TM, Van Steveninck J (1981) Photodynamic protein cross-linking. Biochim Biophys Acta 647:87–94

Waksman R, McEwan PE, Moore TI, Pakala R, Kolodgie FD, Hellinga DG, Seabron RC, Rychnovsky SJ, Vasek J, Scott RW, Virmani R (2008) Photopoint photodynamic therapy promotes stabilization of atherosclerotic plaques and inhibits plaque progression. J Am Coll Cardiol 52:1024–1032

Wilkinson F, Helman WP, Ross AB (1995) Rate constants for the decay and reactions of the lowest electronically excited singlet state of molecular oxygen in solution. An expanded and revised compilation. J Phys Chem Ref Data 24:663–1021

Woodburn KW, Fan Q, Kessel D, Wright M, Mody TD, Hemmi G, Magda D, Sessler JL, Dow WC, Miller RA, Young SW (1996) Phototherapy of cancer and atheromatous plaque with texaphyrins. J Clin Laser Med Surg 14:343–348